Commun. Comput. Phys.
doi: 10.4208/cicp.190612.010313a

Vol. **14**, No. 5, pp. 1287-1303
November 2013

Weighted Interior Penalty Method with Semi-Implicit Integration Factor Method for Non-Equilibrium Radiation Diffusion Equation

Rongpei Zhang[1,3,*], Xijun Yu[2], Jiang Zhu[3], Abimael F. D. Loula[3] and Xia Cui[2]

[1] *School of Sciences, Liaoning ShiHua University, Fushun 113001, China.*
[2] *Laboratory of Computational Physics, Institute of Applied Physics and Computational Mathematics, Beijing 100088, China.*
[3] *Laboratório Nacional de Computação Científica, MCTI, Avenida Getúlio Vargas 333, 25651-075 Petrópolis, RJ, Brazil.*

Received 19 June 2012; Accepted (in revised version) 1 March 2013

Communicated by Ming-Chih Lai

Available online 13 June 2013

Abstract. Weighted interior penalty discontinuous Galerkin method is developed to solve the two-dimensional non-equilibrium radiation diffusion equation on unstructured mesh. There are three weights including the arithmetic, the harmonic, and the geometric weight in the weighted discontinuous Galerkin scheme. For the time discretization, we treat the nonlinear diffusion coefficients explicitly, and apply the semi-implicit integration factor method to the nonlinear ordinary differential equations arising from discontinuous Galerkin spatial discretization. The semi-implicit integration factor method can not only avoid severe timestep limits, but also takes advantage of the local property of DG methods by which small sized nonlinear algebraic systems are solved element by element with the exact Newton iteration method. Numerical results are presented to demonstrate the validity of discontinuous Galerkin method for high nonlinear and tightly coupled radiation diffusion equation.

AMS subject classifications: 35R05, 35Q79, 65M60, 80A20

Key words: Discontinuous Galerkin, weighted interior penalty, semi-implicit integration factor, non-equilibrium radiation diffusion.

1 Introduction

Non-equilibrium radiation diffusion systems have been used to simulate problems in inertial confinement fusion, Z-pinch experiments, and astrophysical problems [1–3]. From

*Corresponding author. *Email addresses:* rpzhang@lncc.br (R. Zhang), yuxj@iapcm.ac.cn (X. Yu), jiang@lncc.br (J. Zhu), aloc@lncc.br (A. Loula), cui_xia@iapcm.ac.cn (X. Cui)

the standpoint of partial differential equations, these systems are highly nonlinear and tightly coupled and exhibit multiple time and space scales.

In recent years, a great deal of literatures gave various numerical algorithms for the non-equilibrium radiation diffusion systems. Mostly of them are finite volume method. Knoll et al. have studied this problem in a series of papers [4–8]. Sheng et al. constructed a monotone finite volume scheme on distorted meshes for multimaterial non-equilibrium radiation diffusion equations [9], then applied the Picard iteration to the nonlinear algebraic systems. Yuan et al. presented the recent progress in numerical methods for radiation diffusion equation [10]. Their works focus on the construction of the nonlinear solver for the large nonlinear algebraic systems. Recently, Yue et al. proposed Picard-Newton iterative method to avoid the low efficiency of Picard iteration [11].

The finite element methods were also applied to the radiation diffusion systems. Mavriplis discretized the radiation diffusion systems by standard finite element method and employed the multigrid method to the nonlinear systems [12]. Kang presented P_1 nonconforming finite element for the radiation equation [13]. However, whether the finite element method or the nonconforming finite element method, they are not "local" method because the load vector will involve the nearest neighbor stencil. Their methods comprise a non-linear solver which is used to solve the non-linear equations directly and a linear solver which is used to solve the linear system arising from the linearization of the non-linear system.

In this paper, we present a weighted discontinuous Galerkin (DG) method for numerically solving radiation diffusion equation. Since their introduction over 30 years ago [14], DG methods have emerged as an attractive tool in various fields because of the flexibility for arbitrarily unstructured meshes, suitability for hp-adaptive implementation, and high parallelizability. For diffusion problems, various DG methods have been analyzed, including local discontinuous Galerkin method (LDG) [15], the diffusive generalized Riemann problem DG method (dGRP) [16, 17], the direct discontinuous Galerkin method (DDG) [18, 19], and interior penalty (IP) method [20]. Recently, Ern et al. [21] proposed weighted interior penalty (WIP) method for advection-diffusion equations with discontinuous diffusivity. The numerical flux in WIP method depends on the harmonic average weight instead of original arithmetic average. Cai et al. proposed three numerical fluxes based on the arithmetic, the harmonic, and the geometric average weight for elliptic interface problems [22]. In this paper, we evaluate the diffusion coefficients as constants on the element center and then construct weighted interior penalty method based on the above three weights.

For the time discretization, the implicit time integration methods rather than explicit methods, are often used for non-equilibrium radiation diffusion equations which have strong nonlinear transients. Previous researches include Knoll et al. [4] who compared three time integration methods: the semi-implicit method, the fully implicit Picard method, and the Newton-Krylov method. Lowrie [23] considered Beam and Warming scheme, Crank-Nicolson scheme, and predictor-corrector scheme etc. and compared the efficiency and accuracy of these methods. Ref. [24] studied linearly implicit and implicitly

balanced method. Mousseau et al. [25] studied a variety of first- and second-order time-integration methods for two-dimensional non-equilibrium radiation diffusion equation and compared their accuracy and efficiency. However the time integration methods mentioned above would introduce large scale algebraic systems which need the construction of linear and nonlinear solvers.

Verwer and Sommeijer have proposed an implicit-explicit (IMEX) Runge-Kutta-Chebyshev (RKC) scheme for radiation diffusion equations in [26]. This is a kind of semi implicit time discretization method. They treat the reaction terms implicitly and diffusion terms explicitly. This decoupling can make sure that the implicit terms have no underlying spatial grid connectivity, then the local nonlinear algebraic systems can be solved by modified Newton method. Although the IMEX RKC method is a local time discretization, it will need a very large number of stages per time step to achieve stability.

The DG method discretizes the spatial variables and leads to a relatively large number of degrees of freedom in comparison to other discretization methods. For example, assuming about the linear triangular elements, the DG systems involves 3 times the number of unknowns of the corresponding finite volume method. Solving these large systems implicitly would cause enormous computational cost. It is essential to construct a suitable time discretization techniques which have good stiffness stability and preserve the "local" property of the DG method. Nie et al. [27] proposed implicit integration factor (IIF) method for the stiff reaction-diffusion equations. A novel feature of IIF method is that the nonlinear algebraic systems can be solved element by element. Then the IIF method can be regarded as a local time discretization. Chen and Zhang [28] developed Krylov implicit integration factor methods for DG spatial discretization on unstructured meshes. However, these calculations depend on the fact that the diffusion coefficients are constant. The main difficulty in implementing integration factor type method is how to treat the nonlinear diffusion coefficients.

In this paper, we address this problem by using the semi-implicit method as in [4, 24] and develop semi-implicit integration factor (SIIF) method to solve the radiation diffusion systems. The idea is to evaluate the nonlinear diffusion coefficients at previous time level n and keep the reaction terms at the present time level $n+1$. There are some difficulties in applying the IF method which require the calculation of exponentials of the matrices. We apply the Krylov subspace method to the computation of the matrix exponential operator as in the [29]. The SIIF method is much easier to implement and demands much less computational effort than the fully implicit time discretization methods. Meanwhile this method can also allow for a large time step size which is proportional to the spatial grid size. The main advantage of this method is that it is a local time discretization method and the nonlinear algebraic systems can be solved element by element.

The outline of the paper is as follows. In Section 2, we present the weighted interior penalty method for the non-equilibrium radiation diffusion systems. The semi-implicit integration factor time discretization scheme is carried out in Section 3. Numerical examples are presented in Section 4. We end our presentation in Section 5 with concluding remarks.

2 Discontinuous Galerkin approximation

2.1 Non-equilibrium radiation diffusion systems

Under the assumption of an optically thick medium, a first-principles statement of radiation transport reduces to the radiation diffusion limit. The idealized dimensionless equation for non-equilibrium diffusion coupled to material conduction, known as the "2T" model, can be written as

$$\frac{\partial E}{\partial t}-\nabla\cdot(D_r\nabla E)=\sigma_a(T^4-E), \tag{2.1}$$

$$\frac{\partial T}{\partial t}-\nabla\cdot(D_t\nabla T)=-\sigma_a(T^4-E). \tag{2.2}$$

The problem consists of two strongly nonlinear diffusion equations with a highly stiff reaction term. The dependent variables are E and T, representing, respectively, radiation energy and material temperature. The energy exchange is controlled by the photon absorption cross section σ_a, which is defined by $\sigma_a=\frac{z^3}{T^3}$. The energy diffusion coefficient D_r with flux limiter is as follows

$$D_r=\frac{1}{3\sigma_a+\frac{|\nabla E|}{E}}, \tag{2.3}$$

where $|\nabla E|$ is the Euclidean norm of the gradient ∇E. The limiter term $\frac{|\nabla E|}{E}$ is an artificial means of ensuring physically meaningful energy propagation speeds (i.e. no faster than the speed of light). In addition to the non-linear behavior resulting from the governing equations, the flux-limited form of the diffusion coefficient introduces an extra degree of non-linearity to the system. The material conduction coefficient is defined as

$$D_t=\kappa T^{\frac{5}{2}}, \tag{2.4}$$

with $\kappa=0.01$. The atomic number z is a material coefficient of being a function of position (x,y).

The computational domain Ω is assumed to be a unit square domain. We represent the boundary $x=0,0\le y\le 1$ and $x=1,0\le y\le 1$ by Γ_0, and otherwise by Γ_1, i.e. that $\partial\Omega=\Gamma_0\cup\Gamma_1$. To be consistent with previous works [13], the boundary conditions are defined as follows:

$$\frac{E}{4}+\frac{1}{6\sigma_a}\frac{\partial E}{\partial n}=g, \quad \text{on } \Gamma_0, \tag{2.5a}$$

$$\frac{\partial E}{\partial n}=0, \quad \text{on } \partial\Omega-\Gamma_0, \tag{2.5b}$$

$$\frac{\partial T}{\partial n}=0, \quad \text{on } \partial\Omega, \tag{2.5c}$$

where n is the local outward normal vector to the boundary.

2.2 Weighted interior penalty method

We consider a triangulation $\mathcal{T}_h$ of Ω which consists of non-overlapping triangles $\mathcal{T}_h = \bigcup_{m=1}^{N_e} \triangle_m$, where N_e denotes the number of triangular elements. We denote by $\mathcal{E}_h = \mathcal{E}_h^{\mathtt{in}} \bigcup \mathcal{E}_h^0 \bigcup \mathcal{E}_h^1$ the set of all edges of $\mathcal{T}_h$ where $\mathcal{E}_h^{\mathtt{in}}$ is the set of all interior edges, and $\mathcal{E}_h^0$ and $\mathcal{E}_h^1$ are the sets of boundary faces belonging to the respective Γ_0 and Γ_1. For each $e \in \mathcal{E}_h$, we denote h_e as the length of the edge e and associate a unit normal vector $\mathbf{n}_e$ to e. Denote h_{min} as the minimum length of all triangular edges. If $e \in \mathcal{E}_h^0 \bigcup \mathcal{E}_h^1$, $\mathbf{n}_e$ is taken to be unit outward vector normal to $\partial\Omega$.

If $e \in \mathcal{E}_h^{\mathtt{in}}$, let $\triangle_1^e$ and $\triangle_2^e$ be the two elements sharing the common edge e, we assume that the normal vector $\mathbf{n}_e$ is oriented from $\triangle_1^e$ to $\triangle_2^e$. There are two traces of function u along e:

$$u_1^e = \{u(x,y):\ (x,y) \in \triangle_1^e,\ (x,y) \to e\}, \qquad u_2^e = \{u(x,y):\ (x,y) \in \triangle_2^e,\ (x,y) \to e\}.$$

Now we define the jump of a function u over edge e as

$$[u] = u_1^e - u_2^e.$$

We also define the following weighted averages

$$\{u\}_w = w_2^e u_1^e + w_1^e u_2^e$$

with the weights satisfying

$$w_2^e \in [0,1], \quad w_1^e \in [0,1], \quad w_2^e + w_1^e = 1. \tag{2.6}$$

We define the DG approximation space as

$$V_h = \{v \in L^2(\Omega):\ v|_{\triangle_m} \in P^k(\triangle_m),\ m = 1,2\cdots,N_e\}. \tag{2.7}$$

where $P^k(\triangle_m)$ denotes the space of polynomials of total degree less than or equal to k on element $\triangle_m$. Then the weighted interior penalty DG method is defined as follows, find $E, T \in V_h$, such that

$$\sum_{m=1}^{N_e} \int_{\Delta_m} E_t \phi dxdy + a_\theta(E,\phi) = \sum_{m=1}^{N_e} \int_{\Delta_m} \sigma_a (T^4 - E)\phi dxdy + \sum_{e \in \mathcal{E}_h^0} \int_e 2g\phi ds, \tag{2.8}$$

$$\sum_{m=1}^{N_e} \int_{\Delta_m} T_t \psi dxdy + b_\theta(T,\psi) = -\sum_{m=1}^{N_e} \int_{\Delta_m} \sigma_a (T^4 - E)\psi dxdy, \tag{2.9}$$

for all $(\phi,\psi) \in V_h$. The DG bilinear forms $a_\theta(E,v)$ in (2.8) are defined as

$$\begin{aligned} a_\theta(E,\phi) = &\sum_{m=1}^{N_e} \int_{\Delta_m} D_r \nabla E \cdot \nabla \phi dxdy + \sum_{e \in \mathcal{E}_h^{in}} \int_e \frac{\gamma_\theta}{h_e} W_e [E][\phi] ds + \sum_{e \in \mathcal{E}_h^0} \int_e \frac{E}{2} \phi ds \\ &- \sum_{e \in \mathcal{E}_h^{in}} \int_e \{D_r \nabla E \cdot \mathbf{n}\}_w [\phi] ds + \theta \sum_{e \in \mathcal{E}_h^{in}} \int_e \{D_r \nabla \phi \cdot \mathbf{n}\}_w [E] ds. \end{aligned} \tag{2.10}$$

Note that we approximate the flux $D_r\frac{\partial E}{\partial n}$ by $\frac{1}{3\sigma_a}\frac{\partial E}{\partial n}$ on the boundary $\mathcal{E}_h^0$, the same treatment can be found in [13].

Similarly, we can define the DG bilinear forms $b_\theta(T,\psi)$ in (2.9) as

$$b_\theta(T,\phi)=\sum_{m=1}^{N_e}\int_{\Delta_m}D_t\nabla T\cdot\nabla\psi dxdy+\sum_{e\in\mathcal{E}_h^{in}}\int_e\frac{\gamma_\theta}{h_e}W_e[T][\psi]ds$$
$$-\sum_{e\in\mathcal{E}_h^{in}}\int_e\{D_t\nabla T\cdot\mathbf{n}\}_w[\psi]ds+\theta\sum_{e\in\mathcal{E}_h^{in}}\int_e\{D_t\nabla\psi\cdot\mathbf{n}\}_w[T]ds. \tag{2.11}$$

The penalty parameter γ_θ is set to be a positive constant. The bilinear form (2.8)-(2.9) corresponding to $\theta=-1$, 0, or 1 are the so-called symmetric interior penalty Galerkin (SIPG), incomplete interior penalty Galerkin (IIPG), or nonsymmetric interior penalty Galerkin (NIPG).

There are several possible choices of the weights in (2.10). Let e be the common edge of elements $\triangle_1^e$ and $\triangle_2^e$: $e=\triangle_1^e\bigcap\triangle_2^e$. Denote by $D_{r,1},D_{r,2}$ as the values of D_r on the center of triangles $\triangle_1^e$ and $\triangle_2^e$. There are three choices of the weights $w_{1,2}^e$: the arithmetic weight, the harmonic weight, and the geometric weight [22]

$$w_1^e=\frac{1}{2},\qquad w_2^e=\frac{1}{2}, \tag{2.12a}$$
$$w_1^e=\frac{D_{r,2}}{D_{r,1}+D_{r,2}},\qquad w_2^e=\frac{D_{r,1}}{D_{r,1}+D_{r,2}}, \tag{2.12b}$$
$$w_1^e=\frac{\sqrt{D_{r,2}}}{\sqrt{D_{r,1}}+\sqrt{D_{r,2}}},\quad w_2^e=\frac{\sqrt{D_{r,1}}}{\sqrt{D_{r,1}}+\sqrt{D_{r,2}}}. \tag{2.12c}$$

Then W_e is the corresponding arithmetic, harmonic, and geometric averages on edge e:

$$W_{e,a}=\frac{D_{r,1}+D_{r,2}}{2},\quad W_{e,h}=\frac{2D_{r,1}D_{r,2}}{D_{r,1}+D_{r,2}},\quad W_{e,g}=\sqrt{D_{r,1}D_{r,2}}. \tag{2.13}$$

These averages satisfy the following relations: $W_{e,h}\le W_{e,g}\le W_{e,a}$. The weights and averages in (2.11) are defined similarly. With the choices of weights in (2.13), the corresponding DG methods in (2.8)-(2.9) are called the arithmetic, the harmonic, and the geometric weighted interior penalty methods, respectively.

In this paper, we consider the linear element. The basis function on each element is the linear function ϕ_i, $i=1,2,3$ which takes the value 1 at the midpoint of the ith edge and the value 0 at the mid-points of the two other edges. The approximate solution on element Δ_m can be represented by

$$E=\sum_{i=1}^{3}E_i\phi_i(x,y), \tag{2.14}$$

where the degrees of freedom E_i are values of the numerical solution at the midpoints of the ith edge. To perform the integration in space, we use the three mid-point rule on each triangle in $\mathcal{T}_h$. Hence the mass matrix on every triangle can be obtained by

$$\int_{\Delta_m} \phi_i \phi_j dxdy = \frac{|\Delta_m|}{3}\delta_{ij}, \quad i,j=1,2,3. \tag{2.15}$$

And because ∇E is a piecewise constant on each triangle, we can compute the ∇E needed in D_r exactly. Also, the volume integral for the nonlinear parts in (2.8) can be approximated by

$$\int_{\Delta_m} \sigma_a (T^4 - E)\phi_i dxdy = \frac{|\Delta_m|}{3} z^3 (T_i - \frac{E_i}{T_i^3}), \quad i=1,2,3 \tag{2.16}$$

due to the properties of the basis functions. So we can easily compute the Jacobian in the Newton iteration, as it will be shown in (3.9).

3 Semi-implicit integration factor time discretization

In this section, we first propose the SIIF method for the nonlinear ODEs generated by the DG spacial discretization. Then we use the Newton method to solve the small nonlinear algebraic system on every triangular element.

Denote Δt as the time step and the superscript n as the time levels. To perform the semi-implicit integration factor method in time, we write the semi-discrete schemes (2.8)-(2.9) into the following global nonlinear ODE system by inverting the mass matrix:

$$\frac{d\mathbf{U}}{dt} = \mathbf{A}(\mathbf{U})\mathbf{U} + \mathbf{F}(\mathbf{U}), \tag{3.1}$$

where $\mathbf{U} = (\mathbf{U}_1^T, \mathbf{U}_2^T, \cdots, \mathbf{U}_{N_e}^T)^T$ is the vector of unknowns containing the degrees of freedom of E and T on every element with $\mathbf{U}_m^T = (E_1, E_2, E_3, T_1, T_2, T_3)_m$. The stiffness matrix $\mathbf{A}(\mathbf{U})$ is the nonlinear global sparse matrix which is determined by the nonlinear diffusion coefficients D_r and D_t. The right hand side $\mathbf{F}(\mathbf{U}) = (\mathbf{F}_1^T, \mathbf{F}_2^T, \cdots, \mathbf{F}_{N_e}^T)^T$, where each term $\mathbf{F}_m^T$ can be computed by (2.16) and boundary condition. Note that the superscript ^{T} in the above formula represent the matrix transposition.

There are two difficulties in applying the implicit integration factor method for the nonlinear radiation diffusion equation. The first obstacle is that the global matrix $\mathbf{A}(\mathbf{U})$ depends on the nonlinear diffusion coefficients D_r and D_t. To overcome this obstacle, a commonly used approach for radiation diffusion system is referred to as the semi-implicit method [4]. In the semi-implicit method, the radiation diffusion coefficients D_r and D_t are evaluated at time level n. In this way we get following ODE system:

$$\frac{d\mathbf{U}}{dt} = \mathbf{A}(\mathbf{U}^n)\mathbf{U} + \mathbf{F}(\mathbf{U}). \tag{3.2}$$

The matrix $\mathbf{A}(\mathbf{U}^n)$ can be thought as a constant matrix, we multiply (3.1) by the integration factor $e^{-\mathbf{A}(\mathbf{U}^n)t}$ and integrate over one time step from t^n to t^{n+1} to obtain

$$\mathbf{U}^{n+1}=e^{\mathbf{A}(\mathbf{U}^n)\Delta t}\mathbf{U}^n+e^{\mathbf{A}(\mathbf{U}^n)\Delta t}\int_0^{\Delta t}e^{\mathbf{A}(\mathbf{U}^n)\tau}\mathbf{F}(\mathbf{U}(t^n+\tau))d\tau. \tag{3.3}$$

The integrand in (3.2) can be approximated by using an $r-1$th order Lagrange interpolation polynomial with interpolation points at $t^{n+1},t^n,\cdots,t^{n+2-r}$. Then we obtain the rth order scheme

$$\mathbf{U}^{n+1}=e^{\mathbf{A}(\mathbf{U}^n)\Delta t}\mathbf{U}^n+\Delta t\left(\alpha_1\mathbf{F}(\mathbf{U}^{n+1})+\sum_{i=0}^{r-2}\alpha_{-i}e^{(i+1)\mathbf{A}(\mathbf{U}^n)\Delta t}\mathbf{F}(\mathbf{U}^{n-i})\right), \tag{3.4}$$

see [27] for the values of coefficients α_j for schemes with different orders. In this paper we use the following second order semi-implicit integration factor scheme

$$\mathbf{U}^{n+1}=e^{\mathbf{A}(\mathbf{U}^n)\Delta t}(\mathbf{U}^{\mathbf{n}}+\frac{\triangle t}{2}\mathbf{F}(\mathbf{U}^n))+\frac{\triangle t}{2}\mathbf{F}(\mathbf{U}^{n+1}),\quad n=0,1,\cdots. \tag{3.5}$$

The second obstacle in implementing IF method for high dimensional problems lies in the significantly expensive storage and calculation of exponentials of the matrixes, $e^{\mathbf{A}(\mathbf{U}^n)\Delta t}$. Although the discretization matrix are sparse, their exponentials matrix will be dense. So it is not practical to compute and store the exponentials matrix directly. We address this problem by using the Krylov subspace approximations to the products of the exponential matrix and vector, instead of computing the full exponential matrix itself. The underlying principle is to approximate the product $\mathbf{w}=e^{\mathbf{A}(\mathbf{U}^n)\Delta t}\mathbf{v}$ by an element of the Krylov subspace $\mathbf{K}_m(\triangle t,\mathbf{v})=span\{\mathbf{v},\mathbf{A}(\mathbf{U}^n)\Delta t\mathbf{v},\cdots,(\mathbf{A}(\mathbf{U}^n)\Delta t)^{m-1}\mathbf{v}\}$. The dimension m of the Krylov subspace is much smaller than the dimension of the large sparse matrix $\mathbf{A}(\mathbf{U}^n)$. We take $m=25$ in all numerical computations of this paper. The approximation being used is

$$e^{\mathbf{A}(\mathbf{U}^n)\Delta t}\mathbf{v}=\beta\mathbf{V}_{m+1}e^{\triangle t\overline{\mathbf{H}}_{m+1}}\mathbf{e}_1, \tag{3.6}$$

where $\mathbf{e}_1$ is the first unit basis vector, $\beta=\|\mathbf{v}\|_2$; $\mathbf{V}_{m+1}=(\mathbf{v}_1,\cdots,\mathbf{v}_{m+1})$ and $\overline{\mathbf{H}}_{m+1}=[h_{ij}]$ are, respectively, the orthonormal basis and the upper Hessenberg matrix resulting from the following well-known Arnoldi process:

Algorithm 3.1

$\overline{\mathbf{H}}_{m+2}=zeros[m+2,m+2]$;

1. Compute the initial vector: $\mathbf{v}_1=\mathbf{v}/\|\mathbf{v}\|_2$;
2. Perform iterations: Do $j=1,2,\cdots,m$:
   (1) Compute the vector $\mathbf{p}=\mathbf{A}(\mathbf{U}^n)\mathbf{v}_j$;
   (2) Do $i=1,2,\cdots,j$:

(2.1) Compute the inner product $h_{ij}=(\mathbf{p},\mathbf{v}_i)$;

(2.2) Compute the vector $\mathbf{p}=\mathbf{p}-h_{ij}\mathbf{v}_i$;

(3) Compute $h_{j+1,j}=\|\mathbf{p}\|_2$;

(4) If $h_{j+1,j}=0$, then stop the iteration;

Else compute the next basis vector $\mathbf{v}_{j+1}=\mathbf{p}/h_{j+1,j}$.

3. $\overline{\mathbf{H}}(m+2,m+1)=1$.

In this paper we get the approximation of the product by means of the software package EXPOKIT developed by Sidge [29].

Applying the Krylov subspace approximation (3.6) to (3.5), we obtain the second order semi-implicit IF schemes

$$\mathbf{U}^{n+1}=\beta^n\mathbf{V}^n_{m+1}e^{\triangle t\overline{\mathbf{H}}^n_{m+1}}\mathbf{e}_1+\frac{\triangle t}{2}\mathbf{F}(\mathbf{U}^{n+1}),\quad n=0,1,\cdots. \tag{3.7}$$

where $\beta^n=\|\mathbf{U^n}+\frac{\triangle t}{2}\mathbf{F}(\mathbf{U}^n)\|_2$, $\mathbf{V}^n_{m+1}$ and $\mathbf{H}^n_{m+1}$ are generated by the above Arnoldi algorithm with the initial vector $\mathbf{U^n}+\frac{\triangle t}{2}\mathbf{F}(\mathbf{U}^n)$ and the sparse matrix $\mathbf{A}(\mathbf{U}^n)$. This semi-implicit IF scheme (3.7) separates the right hand sides into explicit and implicit parts. If we assume that $\mathbf{Q}^n=\beta^n\mathbf{V}^n_{m+1}e^{\triangle t\overline{\mathbf{H}}^n_{m+1}}\mathbf{e}_1$, where $\mathbf{Q}=(\mathbf{Q}_1^T,\mathbf{Q}_2^T,\cdots,\mathbf{Q}_{N_e}^T)^T$. Then we can get the following local nonlinear algebraic system

$$\mathbf{R}(\mathbf{U}^{n+1}_m)=\mathbf{U}^{n+1}_m-\mathbf{Q}^n_m-\frac{\triangle t}{2}\mathbf{F}_m(\mathbf{U_m}^{n+1})=0,\quad m=1,\cdots,N_e. \tag{3.8}$$

We solve the nonlinear systems (3.8) element by element by the following Newton iteration algorithm.

Algorithm 3.2

Give the initial value $\mathbf{U}^0_m$ and compute $\mathbf{U}^{n+1}_m$ from $\mathbf{U}^n_m$ for $m=1,2,\cdots N_e$.

1. $\mathbf{U}^{n+1,0}_m=\mathbf{U}^n_m$.
2. Compute the Jacobi matrix $\mathbf{J}$ of $\mathbf{R}(\mathbf{U}^{n+1,k}_m)$ and solve the algebraic systems: $\mathbf{J}\mathbf{S}^{k+1}=-\mathbf{R}(\mathbf{U}^{n+1,k}_m)$, $k=0,1,2,\cdots$.
3. $\mathbf{U}^{n+1,k+1}_m=\mathbf{U}^{n+1,k}_m+\mathbf{S}^{k+1}$.
4. Substituting $\mathbf{U}^{n+1,k+1}_m$ into (3.8) and compute $\mathbf{R}(\mathbf{U}^{n+1,k+1}_m)$,

   If $|\mathbf{R}(\mathbf{U}^{n+1,k+1}_m)|<\epsilon$ is satisfied, then stop and $\mathbf{U}^{n+1}_m=\mathbf{U}^{n+1,k+1}_m$.

   Else $\mathbf{U}^{n+1,k}_m=\mathbf{U}^{n+1,k+1}_m$ and go to step 2.

The threshold value ϵ for judging Newton iteration convergence is set to be small enough, we take $\epsilon=10^{-13}$.

For P_1 DG finite element, the corresponding Jacobi matrix J in Algorithm 3.2 can be easily calculated. We omit the subscript m for simplicity in the following matrix form.

$$\begin{pmatrix} 1+\frac{\Delta t}{2}\frac{z^3}{T_1^3} & 0 & 0 & -\frac{\Delta t}{2}z^3\left(1+\frac{3E_1}{T_1^4}\right) & 0 & 0 \\ 0 & 1+\frac{\Delta t}{2}\frac{z^3}{T_2^3} & 0 & 0 & -\frac{\Delta t}{2}z^3\left(1+\frac{3E_2}{T_2^4}\right) & 0 \\ 0 & 0 & 1+\frac{\Delta t}{2}\frac{z^3}{T_3^3} & 0 & 0 & -\frac{\Delta t}{2}z^3\left(1+\frac{3E_3}{T_3^4}\right) \\ -\frac{\Delta t}{2}\frac{z^3}{T_1^3} & 0 & 0 & 1+\frac{\Delta t}{2}z^3\left(1+\frac{3E_1}{T_1^4}\right) & 0 & 0 \\ 0 & -\frac{\Delta t}{2}\frac{z^3}{T_2^3} & 0 & 0 & 1+\frac{\Delta t}{2}z^3\left(1+\frac{3E_2}{T_2^4}\right) & 0 \\ 0 & 0 & -\frac{\Delta t}{2}\frac{z^3}{T_3^3} & 0 & 0 & 1+\frac{\Delta t}{2}z^3\left(1+\frac{3E_3}{T_3^4}\right) \end{pmatrix} \tag{3.9}$$

Remark 3.1. Though we have not presented a numerical analysis, we would like to add some comments concerning stability and accuracy of the proposed method. In the all numerical experiments that we have performed we do not observed any stability problem such as blow up or spurious oscillation of the numerical solution. This robust behavior is due to the good stability and local properties of the DG finite element approximation combined with the semi-implicit time integration method adopted here.

Remark 3.2. Concerning the choice of integration time step, in the examples considered here, we have observed that accuracy is more critical than stability. Since we have adopted a semi-implicit scheme with a linearization of the diffusion coefficients on each time step, for the proposed SIIF DG method with P_1 elements we may expect first order approximation in time and second order approximation in space in L_2 norm. The numerical results presented in next in Section 4.1 is in agreement with this conjecture. A complete mathematical and numerical analysis of the model problem addressed here will be presented in future works.

4 Numerical tests

In this section we will study the performance of the P^1 weighted incomplete interior penalty Galerkin method ($\theta = 0$) for the non-equilibrium radiation diffusion problems. Since these equations have no analytic solutions, we first consider a nonlinear parabolic problem with analytic solution to give a convergence test and computational cost. Then we will demonstrate our method on two test problems about non-equilibrium radiation diffusion problems (2.1)-(2.2).

4.1 Numerical examples with analytic solution

Example 4.1. Consider the following nonlinear parabolic equation with the mixed boundary condition

$$u_t - \nabla\cdot(u\nabla u) = f(x,y,t) \quad \text{in } \Omega, \tag{4.1a}$$

$$u = e^{-\pi^2 t}(2+\cos(\pi x)\cos(\pi y)) \quad \text{on } \partial\Omega_S \bigcup \partial\Omega_N, \tag{4.1b}$$

$$u\nabla u\cdot\mathbf{n} = 0 \quad \text{on } \partial\Omega_E \bigcup \partial\Omega_W, \tag{4.1c}$$

where $\Omega=(0,1)\times(0,1)$. The exact solution for (4.1) is $u=e^{-\pi^2 t}(2+\cos(\pi x)\cos(\pi y))$. The initial condition and right hand side $f(x,y,t)$ are determined by the exact solution. This example has been used as a convergence test by Sheng [30] in which the fully implicit scheme was adopted with time step $\Delta t = 10^{-5}$. We use the SIPG method on various triangular meshes for spatial discretization, and the SIIF method for time integration with a uniform time step $\Delta t = 5\times 10^{-6}$. The time step is sufficiently small so that the spatial error dominates the computation. The computation is carried up to $t=0.01$ with the dimension of the Krylov subspace $m=25$. We give the CPU time, errors and order of accuracy for four different levels meshes in Table 1 at time $t=0.01$. From this table, we can get the second-order convergence for the maximum and L_2 norm error. Also, as shown in the CPU time of the numerical tables, we can see that the computations are very efficient. The CPU time approximately increases 4 times when the spatial mesh is refined once. So the CPU time approximately depends linearly on the number of degrees of freedom.

Table 1: CPU time, errors and order of convergence for Example 4.1.

Ne	CPU(s)	L_2 error	Order	L_∞ error	Order
112	4.88	5.66E-3	-	$1.42E-2$	-
394	14.18	1.54E-3	1.87	$4.92E-3$	1.53
1460	50.00	4.48E-4	1.78	$1.25E-3$	1.98
5816	197.93	1.16E-4	1.95	$3.15E-4$	1.98

4.2 Application to non-equilibrium radiation diffusion equation

The weighted DG method with SIIF time discretization will now be demonstrated on two classical model problems to test the validity of this method. The numerical results will be presented in the form of contour and 3D views of radiation temperature which is defined by $T_r = E^{0.25}$.

Example 4.2. We first consider a two-dimensional problem (2.1)-(2.2) with Robin boundary condition (2.5). This model describes a unit radiation flux impinging on an initially cold slab. It includes two cases with only difference between the problems being homogeneity. One case is homogeneous material in which the atomic number z is constant and equal to 1.0 everywhere. The other one is heterogeneous material with the atomic

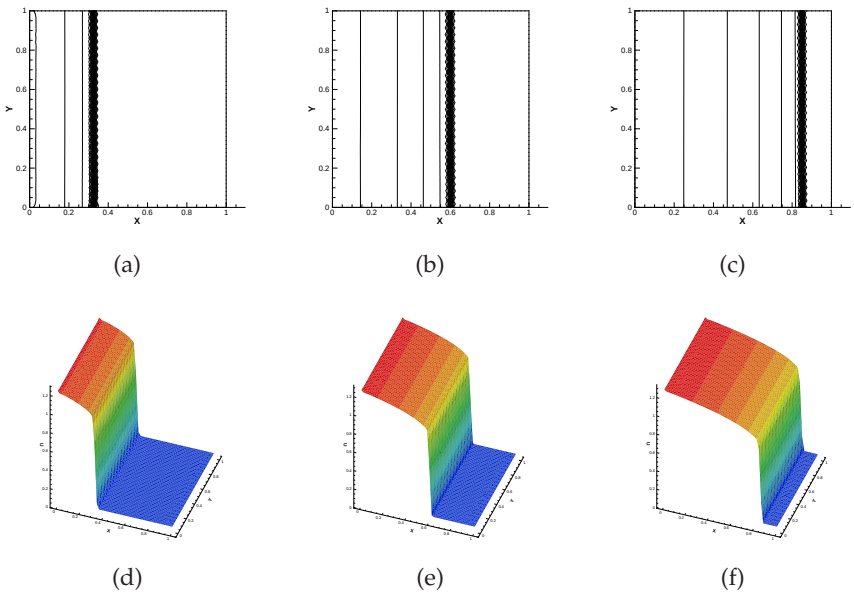

(a) (b) (c)

(d) (e) (f)

Figure 1: Contours and 3D views of radiation temperature of Example 4.2, Case 1 at $t=1$, $t=2$, and $t=3$ (from left to right).

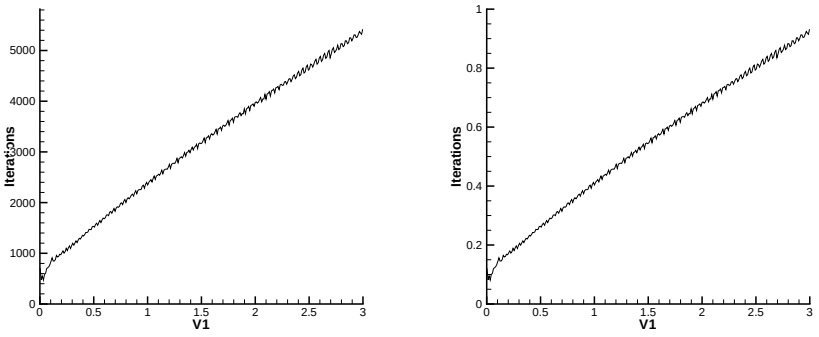

(a) (b)

Figure 2: (a) The sum of Newton iterations on all elements, and (b) the averages of Newton iterations on each element for Example 4.2, Case 1.

number, z, a function of x and y. In the two cases, we use the same initial conditions with $E^0=1.0\times10^{-5}$, $T^0=(E^0)^{0.25}$.

Case 1, the two-dimensional homogeneous problem, is the same with the one-dimensional physics as in [4]. The domain is discretized using a triangular grid containing 5816 triangles. We apply the three weights in scheme (2.8)-(2.9) and get the similar results. In Fig. 1, we plot the contours and 3D view of the radiation temperature T_r at $t=1.0$, $t=2.0$, $t=3.0$ based on the geometric weight. Fig. 1 show that the contours of

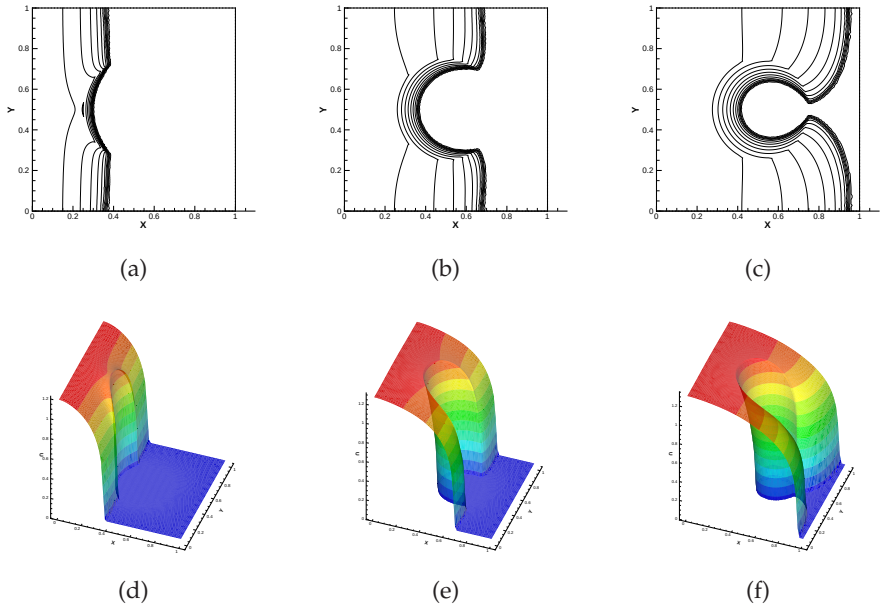

Figure 3: Contours and 3D views of radiation temperature of Example 4.2, Case 2 at $t=1$, $t=2$, and $t=3$ (from left to right).

temperature propagate parallel to the inlet boundary and reproduce the propagation of this one-dimensional phenomenon [6].

In the numerical experiment of Case 1, the time step size is set as $\Delta t = C * h_{min}$ where C is taken to be 0.2. We plot the sum of iterations on all elements and the averages of iterations on each element in Fig. 2. We can see that the iterations gradually increase as the thermal front propagates through the unit square. The Fig. 2(b) also show that the average Newton iteration on each element is no larger than 2.

For Case 2, we consider a unit square domain of two dissimilar materials, where the outer region contains an atomic number of $z=1$ and the inner circular regions ($r \leq 0.25$, with $r=\sqrt{(x-0.5)^2+(y-0.5)^2}$) contains an atomic number of $z=10$. This problem was chosen to demonstrate how the method behaves when faced with a strong spatial dependence of the radiation diffusion coefficient. Fig. 3 show the contour and 3D view of the radiation temperature T_r at $t=1$, $t=2$, and $t=3$, respectively. At the beginning, as the energy propagates, temperature rapidly change near the front. When the thermal front propagates to the layer where the two different materials meet, the progress is impeded by the region of higher atomic number z. At critical times in the simulation, the diffusion coefficients can vary up to six orders of magnitude near the material interfaces. Results show that the method works just as well in heterogeneous as it did in homogeneous case.

Example 4.3. The second model problem we are going to solve is taken from [9]. We solve this problem on the unit square domain which contains two dissimilar materials. The

value for z is 1 everywhere, except in the two inner square regions $\frac{3}{16}<x<\frac{7}{16}$, $\frac{9}{16}<y<\frac{13}{16}$ and $\frac{9}{16}<x<\frac{13}{16}$, $\frac{3}{16}<y<\frac{7}{16}$ where the value for z is 10. As opposed to the first model problem, we consider the solid wall boundary conditions for E and T, namely, all the four walls are insulated with respect to radiation diffusion and material conduction:

$$D_r\nabla E\cdot\mathbf{n}=0,\qquad D_t\nabla T\cdot\mathbf{n}=0. \tag{4.2}$$

Remark 4.1. The solid wall boundary conditions (4.2), which is different with (2.5), will lead to corresponding changes in the DG scheme (2.8) and (2.9). The terms $\sum_{e\in\mathcal{E}_h^0}\int_e 2g\phi ds$ and $\sum_{e\in\mathcal{E}_h^0}\int_e\frac{E}{2}\phi ds$ in (3.8) will be omitted.

The initial radiation energy is given by

$$E^0=1.0\times10^{-3}+100\exp\left(-\left(\frac{r}{0.1}\right)^2\right), \tag{4.3}$$

where $r=\sqrt{x^2+y^2}$. The initial material temperature is defined as in Case 1, i.e. that $T^0=(E^0)^{0.25}$. The computational domain is discretized into unstructured triangular elements with 23274 triangles. Because there are 6 unknown variables on each elements for DG scheme, the number of degrees of freedom of this problem is $6\times23274=139644$. If we solve the problem by the fully implicit scheme, the computation and storage costs are very expensive. On the contrary, the SIIF method can assure that the nonlinear algebraic system can be computed element by element.

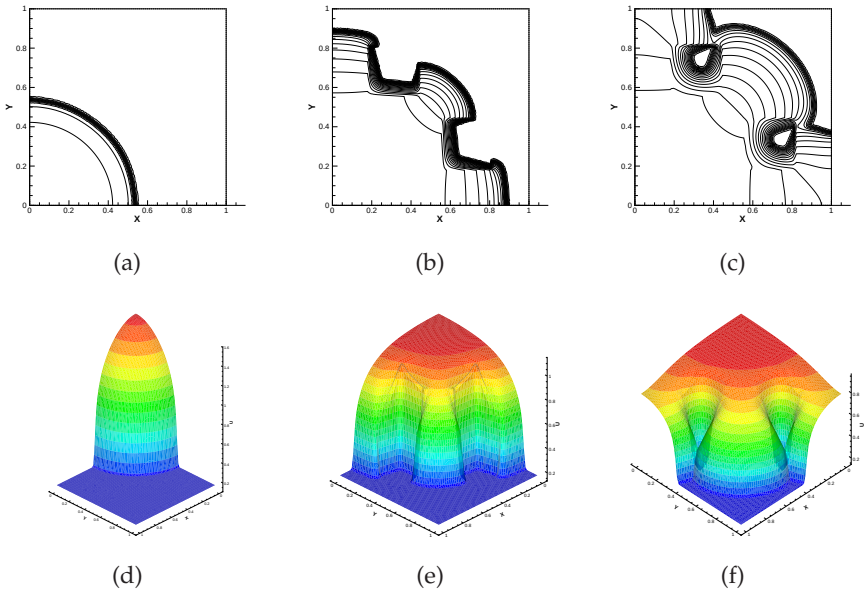

Figure 4: Contours and 3D views of radiation temperature of Example 4.3 at $t=0.5$, $t=1.5$, and $t=3$ (from left to right).

In Fig. 4 the contours and 3D views of radiation temperature are shown at time $t=0.5$, $t=1.5$ and $t=3$, respectively. We have observed that the solution of the SIIF DG method is very close to the solution presented in [9] using a finite volume method. Additionally, we have also observed great accuracy and robustness of the SIIF DG solutions with no spurious oscillation and preserving positivity of E and T approximations, differently from other methods which are unable to preserve this important property (see [9]).

5 Conclusions

We have presented an new numerical method for the solution of non-equilibrium radiation diffusion systems. This method is based on the space discretization by the weighted interior penalty method, and the time discretization by semi-implicit integration factor method. The DG method is shown to resolve very sharp changes of temperature on heterogeneous domains. The semi-implicit integration factor method proved to be an efficient temporal numerical scheme which not only preserves the DG's local property and parallel flexibility but also avoids strict time step restriction required by explicit methods. The obtained results confirm that our DG method is a powerful and reliable method for the numerical solution of nonlinear diffusion problems.

Acknowledgments

R. Zhang and X. Yu's works were partially supported by the National Nature Science Foundation of China (11171038), and R. Zhang's work was also supported by Brazilian Young Talent Attraction Program via National Council for Scientific and Technological Development (CNPq). J. Zhu and A. Loula's works were partially supported by CNPq. X. Cui's work was partially supported by the National Natural Science Foundation of China (11271054), the Science Foundation of CAEP (2010A0202010, 2012B0202026) and the Defense Industrial Technology Development Program (B1520110011). The authors would like to thank the referees for their valuable comments and suggestions.

References

[1] R.L. Bowers, J.R. Wilson, Numerical Modeling in Applied Physics and Astrophysics, Jones and Bartlett, Boston Publishers, 1991.
[2] A.C. Robinson, C.J. Garasi, Three-dimensional z-pinch wire array modeling with ALEGRA-HEDP, Comput. Phys. Commun. 164 (2004) 408-413.
[3] N.J. Turner, J.M. Stone, A module for radiation hydrodynamic calculations with ZEUS-2D using flux-limited diffusion, Astrophys. J. Suppl. Ser. 135 (2001) 95-107.
[4] D.A. Knoll, W.J. Rider, G.L. Olson, An effcient nonlinear solution method for nonequilibrium radiation diffusion, J. Quantum Spectrosc. Radiat. Transfer 63 (1999) 15-29.

[5] D.A. Knoll, W.J. Rider, and G.L. Olson, Nonlinear convergence, accuracy, and time step control in nonequilibrium radiation diffusion, J. Quant. Spectrosc. Radiat. Transfer 70 (2001) 25-36.
[6] V.A. Mousseau, D.A. Knoll and W.J. Rider, Physics-based preconditioning and the Newton-Krylov method for non-linear-equilibrium radiation diffusion, J. Comput. Phys. 160 (2000) 743-765.
[7] V.A. Mousseau, D.A. Knoll, New physics-based preconditioning of implicit methods for non-equilibrium radiation diffusion, J. Comput. Phys. 190 (2003) 42-51.
[8] S.Y. Kadioglu, D.A. Knoll, R.B. Lowrie, R.M. Rauenzahn, A second order self-consistent IMEX method for radiation hydrodynamics, J. Comput. Phys. 229 (2010) 8313-8332.
[9] Z.Q. Sheng, J.Y. Yue and G.W. Yuan, Monotone finite volume schemes of nonequilibrium radiation diffusion equations on distorted meshes, SIAM J. Sci. Comput. 31 (2009) 2915-2934.
[10] G. W. Yuan, X. D. Hang, Z. Q. Sheng, J. Y. Yue. Progress in numerical methods for radiation diffusion equations. Chinese J. Comput. Phys. 26 (2009) 475-500.
[11] J.Y. Yue, G.W. Yuan, Picard-Newton iterative method with time step control for multimaterial non-equilibrium radiation diffusion problem, Commun. Comput. Phys. 10 (2011) 844-866.
[12] D.J. Mavriplis, Multigrid approaches to non-linear diffusion problems on unstructured meshes, Numer. Linear Algebra Appl. 8 (2001) 499-512.
[13] K.E. Kang, P1 nonconforming finite element multigrid method for radiation transport, SIAM J Sci Comput, 25 (2003) 369-384.
[14] W.H. Reed, T.R. Hill, Triangular mesh methods for the neutron transport equation, Los Alamos Scienfic Laboratory Report, LA2UR2732479, 1973.
[15] B. Cockburn, C. W. Shu. The local discontinuous Galerkin method for time-dependent convection-diffusion systems, SIAM J. Numer. Anal. 35 (1998) 2440-2463.
[16] G. Gassner, F. Lörcher and C. A. Munz. A contribution to the construction of diffusion fluxes for finite volume and discontinuous Galerkin schemes. J. Comput. Phys. 224 (2007) 1049-1063.
[17] F. Lörcher, G. Gassner and C. A. Munz. An explicit discontinuous Galerkin scheme with local time-stepping for general unsteady diffusion equations. J. Comput. Phys. 227 (2008) 5649-5670.
[18] H. Liu, J. Yan. The direct discontinuous Galerkin (DDG) methods for diffusion problems. SIAM J. Numer. Anal. 47 (2009), 675-698.
[19] H. Liu, J. Yan. The direct discontinuous Galerkin (DDG) method for diffusion with interface corrections. Commun. Comput. Phys. 3 (2010) 541-564.
[20] L. Song. Fully discrete interior penalty discontinuous Galerkin methods for nonlinear parabolic equations, Numer. Method Partial. Differ. E. 2010 DOI:10.1002/num.20619.
[21] A. Ern, A. Stephansen and P. Zunino. A discontinuous Galerkin method with weighted averages for advection-diffusion equations with locally small and anisotropic diffusivity. IMA J. Numer. Ana. 29(2) (2009) 235-256.
[22] Z. Cai, X. Ye and S Zhang, Discontinuous Galerkin Finite Element Methods for Interface Problems: A Priori and A Posteriori Error Estimations. SIAM J. Numer. Anal. 49 (2011) 1761-1787.
[23] R.B. Lowrie, A comparison of implicit time integration method for nonlinear relaxation and diffusion, J. Comput. Phys. 196 (2004) 566-590.
[24] D.A. Knoll, R.B. Lowrie, J.E. Morel, Numerical analysis of time integration errors for nonequilibrium radiation diffusion. J. Comput. Phys. 226 (2007) 1332-1347.

[25] V.A. Mousseau, D.A. Knoll, Temporal accuracy of the nonequilibrium radiation diffusion equations applied to two-dimensional multimaterial simulations, Nuclear Science and Engineering. 154 (2006) 174-189.
[26] J.G. Verwer, B.P. Sommeijer, An Implicit-explicit Runge-Kutta-Chebyshev scheme for diffusion-reaction equations, SIAM J. Sci. Comput. 25 (2004) 1824-1835.
[27] Q. Nie, Y.-T. Zhang, R. Zhao, Efficient semi-implicit schemes for stiff systems, J. Comput. Phy. 214 (2006) 521-537.
[28] S. Chen, Y. Zhang, Krylov implicit integration factor methods for spatial discretization on high dimensional unstructured meshes: Application to discontinuous Galerkin methods, J. Comput. Phy. 230 (2011) 4336-4352.
[29] R. B. Sidje, Expokit: Software package for computing matrix exponentials, ACM Trans. Math. Software 24 (1998) 130-156.
[30] G. W. Yuan, Z. Q. Sheng. Analysis of accuracy of a finite volume scheme for diffusion equations on distorted meshes, J. Comput. Phys. 224 (2007) 1170-1189.